Application of a Full-Field Calibration Concept for Parameter Identification of HS-Steel with LS-OPT®

Christian Ilg[1], André Haufe[1], David Koch[1], Nielen Stander[2],
Katharina Witowski[1], Åke Svedin[3] , Mathias Liewald[4]
[1]DYNAmore GmbH, Industriestrasse 2, 70569 Stuttgart, Germany
[2]Livermore Software Technology Corporation,
7374 Las Positas Rd., Livermore, CA 94551, United States
[3]DYNAmore Nordic, Linköping, Sweden
[4]Institut für Umformtechnik, Universität Stuttgart, Holzgartenstrasse17, 70174 Stuttgart

Abstract

In recent years results of digital image correlation (DIC) techniques have significantly improved in terms of accuracy, resolution as well as the speed of experimental strain measurement. The current availability of 2D or even 3D surface strain history during loading allows new approaches in constitutive parameter identification. In addition, localization (Fig 1.) exhibited in the numerical simulation can be integrated with DIC to identify constitutive parameters.

Theoretically the complex deformation of a non-homogeneously deformed specimen, as for instance generated by a dog bone shaped coupon with notch or central hole, may be enough to provide all the necessary data to validate a set of parameters of a given constitutive model. For example during tensile loading of an HS-steel sample each material point may pass through a different strain history and can therefore be used for calibration of the yield locus, flow rule and flow curve of an elasto-plastic constitutive model. However, the sheer amount of data that has to be taken into account and be used for reverse engineering is extremely large which eventually slows down the optimization procedure. Hence the straight forward approach of using the full deformation field to optimize the parameter set of a given model may be extremely expensive to achieve at present.

This paper discusses the main possibilities of using DIC to simplify the approach of constitutive parameter identification. It will be shown how DIC data can be sensibly reduced and therefore the amount of necessary computing time decreases as well. Furthermore improvements in measuring accuracy and optimization strategies for material parameter identification when using LS-OPT will be discussed.

Introduction

The necessity to predict the stress and strain behavior in numerical simulations of new or unknown materials as accurate as possible poses major challenges for the industry. To meet this challenge often many different constitutive parameters for rather complex constitutive models need to be identified. Typically, this may be done through lengthy reverse-engineering strategies on the basis of multiple characterization experiments where various test setups have to be discretized and simulated in the desired spatial discretization [1,2,3,4,5]. For identification of constitutive properties of sheet metal the tensile test is the most common test. Here the measurement data such as force vs. elongation curves obtained from the standard tensile tests serve as the basis for parameter identification in particular to find the flow behavior.
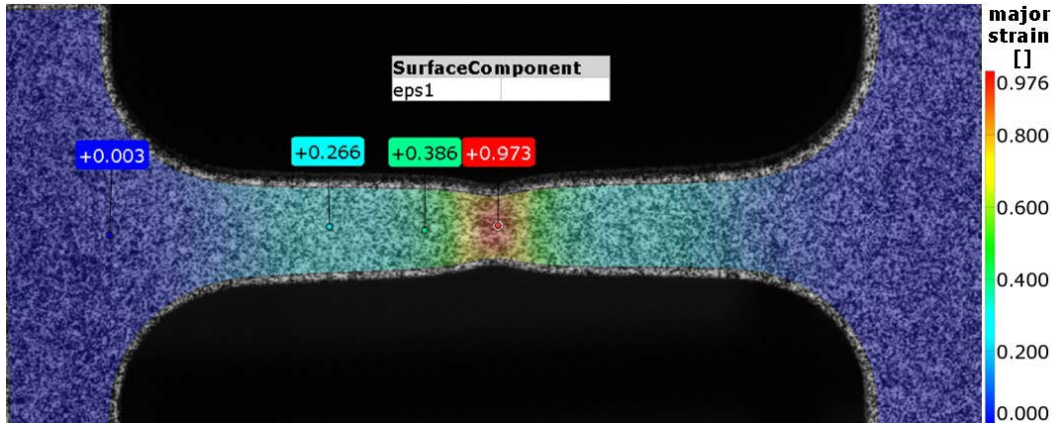

Figure 1: Full-field Measurement of the major strain of a tensile test via DIC.

Due to the undisturbed (or uniform) uniaxial stress state up to uniform elongation the measured force-displacement data can be converted directly into true stress vs. plastic strain data if isochoric behavior is assumed. However, the yield curve obtained by this approach is only valid up to the initiation of necking. Unfortunately this approach disregards the behavior of the specimen in the domain of strain localization within which the straining is typically much higher (see Fig. 1). The behavior within the localization can be studied in more detail using the nominal stress-strain diagram (see Fig. 2). It discloses the variation of curves that are computed based on different reference or gauge lengths. To take the local effects in the necking area into account the displacement field recorded by the optical measurement system may be used. This allows the identification of material parameters based on tensor strain data [6,7,8,9]. In the following, the steps necessary to identify relevant constitutive parameters using full-field displacement measurement data are discussed.
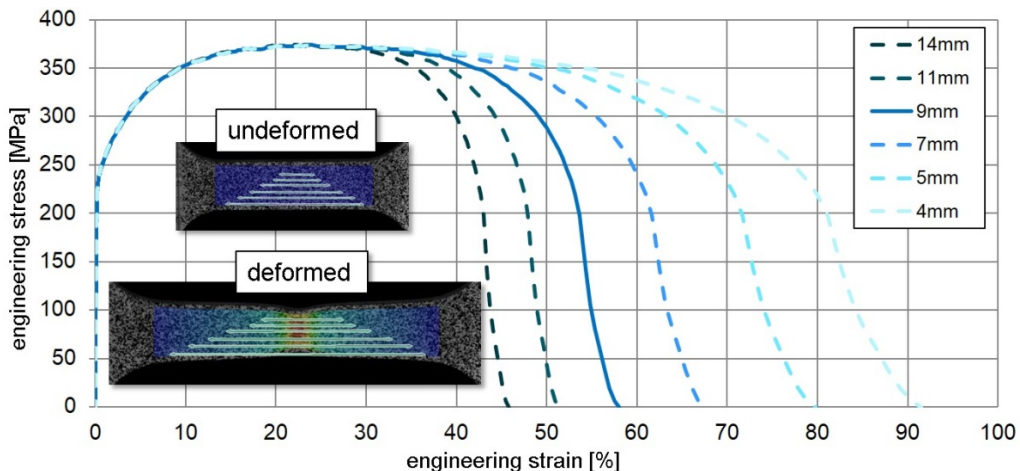

Figure. 2: Strain field measurement via DIC and evaluation of uniaxial engineering strain based on different reference lengths.

Experimental setup

In order to discuss the proposed method in more detail a simple test setup with only a limited number of free parameters has been chosen: Tensile tests of high-strength steel CR210IF are carried out with an electromechanical testing machine. The displacement fields on the surface of the specimen are measured by means of the non-contacting, optical gray scale correlation. For this purpose a stochastic speckle pattern is applied to the targeted domain of the specimen, photographed by two high resolution camera systems and eventually the applied deformations identified through correlation of local points in the pictures adjacent in time. Based on the identified deformation fields, subsequently, the corresponding strain tensors are computed. To identify the sought parameters in a next step local smoothing depending on the used software package may be applied. However, while these technological aspects might influence the calibration procedure to some extend its features are not in the focus of the present paper.

The experimental setup is shown in Fig. 3 (left) and defines the basis of six tensile specimen of the CR210IF sheet metal tested along the rolling direction. The number of six tensile tests only serves to comply with the statistical design of experiments in order to monitor deviations or disturbances. The sample geometry used in this work is called mini flat tensile specimen (MFz). A technical drawing of the specimen is shown in Fig. 3 (right). The chosen geometry has certain advantages: On the one hand, the small number of elements - once spatially discretized for calibration - leads to a shorter computation time of the simulation. On the other hand, due to the smaller measuring volume, the distance between the camera and the specimen can be reduced, thereby improving the resolution of the speckled domain, without missing the necking region. In addition, the middle parallel region of the specimen geometry guarantees a homogeneous stress state despite its smaller area when compared to other test geometries like the standard A80 geometry [10].
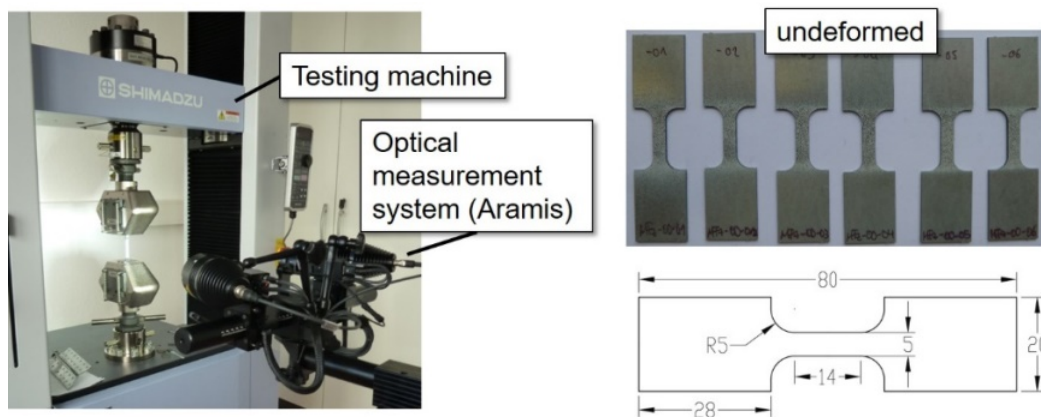

Figure 3: Experimental setup with the testing machine and the optical measurement system on the left and the undeformed specimens with their dimension on the right.

Deformation measurement and computation of the strain field

In the present approach a GOM ARAMIS system has been used to digitize the surface deformation of samples using numerous pictures. For example, in Fig. 4, a picture of the undeformed state of the measured coupon is depicted on the left while a deformed later state in the loading history is shown on the right.
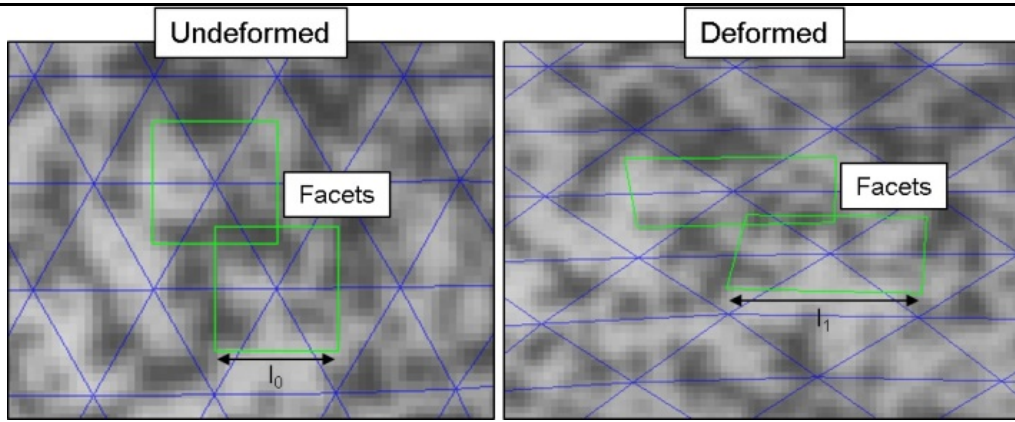
Figure 4: Measuring field and facets in an undeformed (left) and deformed state (right).

Typically, the 3D coordinates of the grid points are determined by the centers of small square image sections (facets) whose size and distance to the next facet center (facet point) can be set and varied. By means of photogrammetry the 3D coordinates of the facet centers are identified using the 2D position on the pictures of the stereo camera system (pictures taken from different angles, left and right). These coordinates can be identified and tracked via the individual and stochastic gray speckle pattern in the different load levels [11]. The 3D position of the facet center is calculated for each load level. Based on the identified facet centers a deformation patch is used to compute the classical deformation tensor F which in turn allows the computation of i.e. logarithmic strain tensor or any other suitable strain measure.

When using the newer ARAMIS versions from 2016 (i.e. the so called professional version), the change of the deformation patch must be taken into account. While in the older versions the strains were computed via a rectangle consisting of eight facet centers, the strains in the new software release are computed using a hexagonal deformation patch. This change results in different reference lengths for the strain calculation (see Fig. 5).

- Reference length in the old software: $l_0 \approx twice\ the\ facet\ point\ distance$
- Reference length in the new software: $l_0 \approx 0{,}75 * twice\ the\ facet\ point\ distance$
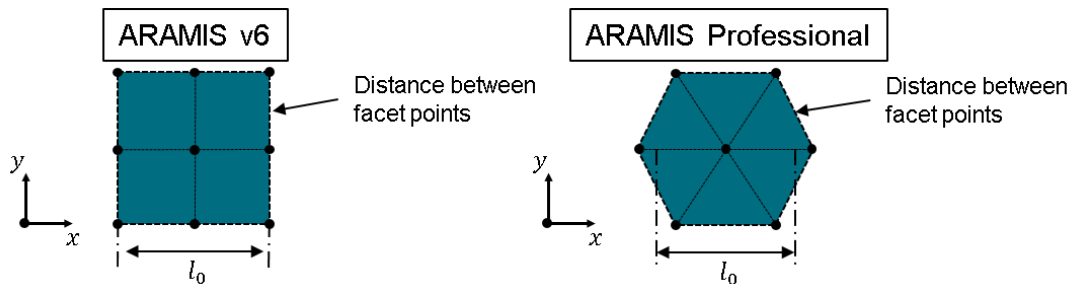

Figure 5: Schematic computation of deformation tensor based on facet patch in the older ARAMIS Software v6 (left) and the newer ARAMIS Software Professional (right).

Numerical model

The principle optimization task that has to be solved needs to focus on the correlation between the measured strain field and the numerically predicted strain field gained from a finite element simulation (see Fig. 6). A big challenge hereby is caused by the fact that both strain fields can be based on different characteristic lengths. While the measured field is computed from the characteristic length of the facet-point field, the numerical simulation delivers strains from the spatial finite element discretization. Clearly, if both length scales are comparable only basic spatial interpolation is necessary.
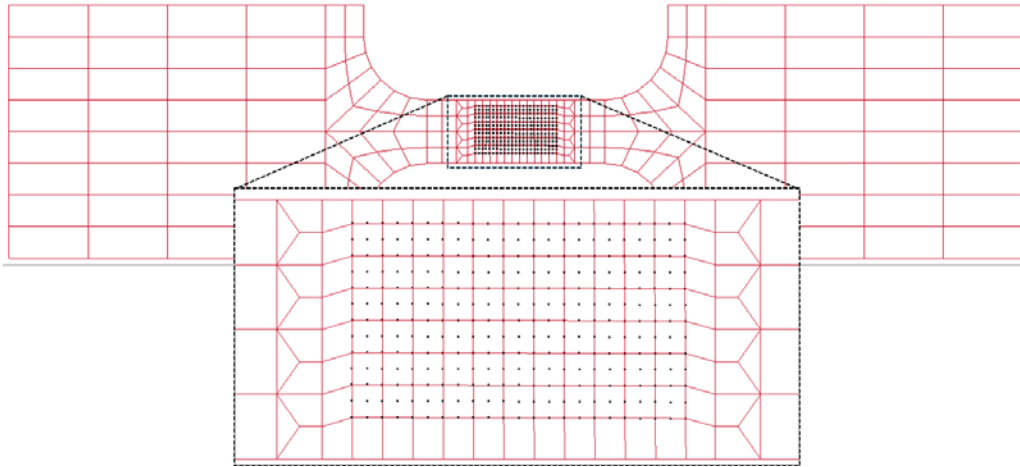
Figure 6: Finite element model of the specimen (red) shown with superimposed optically measured points at the center (black).

However, if these two scales are completely different (i.e. more than a power of ten apart) the yield curve calibration beyond the point of uniform expansion may be questionable. To ensure that the reference length is identical and the data stored on the facet points will be directly projected onto the simulation mesh the geometry from the DIC software can be exported and used for the mesh generation in the finite element model. Standard Tessellation Language (STL) export, which saves the surface as triangles in ASCII format, may be seen as most convenient, as it can be read and imported by LS-PrePost®. In order to generate a finite element mesh on the same basis the triangles may be merged into quadrangular elements and the remains of the geometry outside the DIC domain is built by classical (automated) meshing. Hence comparison of the two strain fields is straight forward.
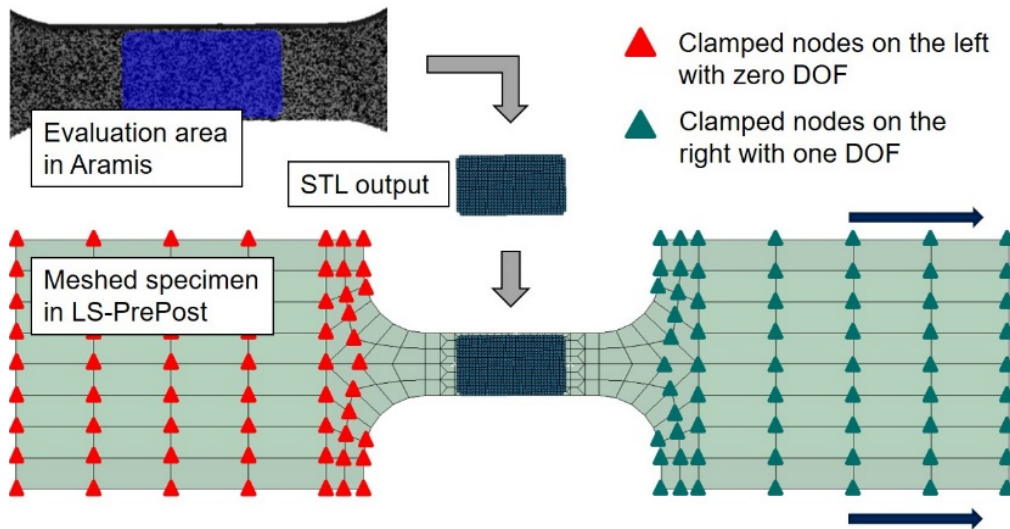

Figure 7: Procedure for creating the mesh in LS-PrePost.

The meshing strategy is shown in Fig. 7. In the upper left corner the overlay of the evaluation domain with the camera image is depicted in blue color. In the center of the picture the STL mesh, exported from DIC can be seen. Below, the geometry and the boundary conditions of the tensile test sample are depicted.

In LS-OPT Ver. 6.0 an option has been implemented which interpolates within the finite element mesh nearest to the facet point. Therefore regular meshes can be used. For the new ARAMIS version this option is mandatory because of the change of the reference length.

Now, the numerical optimization is based on simple J2-plasticity. Here the *von Mises* yield surface, fully associated, is used in the whole domain. For the calculation of the yield curve the elastic part of the technical stress vs. strain curve is subtracted. Thus, the technical stresses and strains can be converted directly into the true (Cauchy) stress and plastic (logarithmic) strain up to the point of uniform elongation due to the homogeneous uniaxial stress state:

$$\sigma_y = \sigma_{eng}(1 + \varepsilon_{eng}) \quad and \quad \varepsilon_{pl} = \ln(1 + \varepsilon_{eng}) - \frac{\sigma_{eng}}{E}$$

Beyond the point of uniform elongation the extrapolation of the yield curve follows the approach of Hockett and Sherby:

$$\sigma_y(\varepsilon_{pl}) = A - Be^{(-c\varepsilon_{pl}^n)}$$

Due to the requirement of *C1*-continuity in the transition from uniform to non-uniform elongation, the Hockett-Sherby equation is being reduced by two parameters, namely *A* and *B* [12].
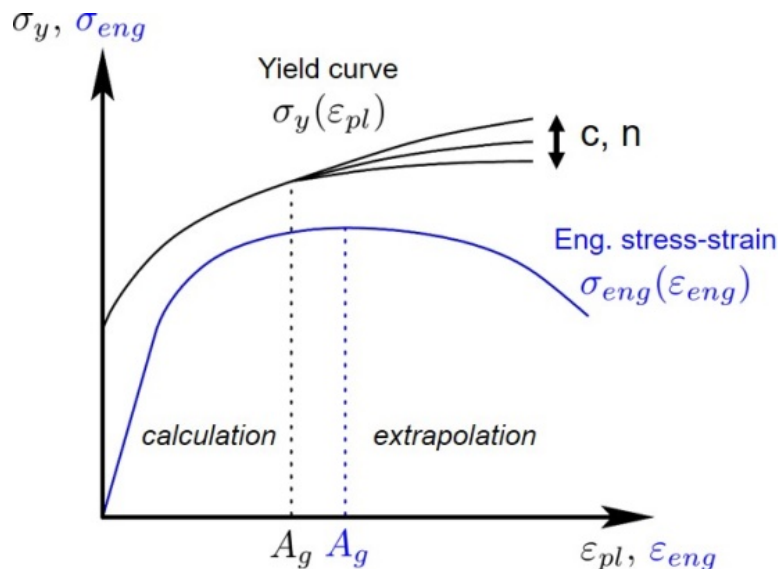

Figure 8: Relationship between the engineering stress-strain curve and the yield curve with an enhanced extrapolation approach.

The remaining parameters *c* and *n* serve furthermore as optimization variables in the numerical optimization procedure controlled by LS-OPT [13]. The creation of the yield curve is shown schematically in Fig. 8. The blue curve, characterized by the elastic part at the start of the course, is an example of a typical engineering stress vs. strain curve from an experimental tensile test. The black curves above show the resulting yield curve with various shapes of the extrapolation. The figure illustrates the removal of the elastic portion, the conversion of the stresses below uniform elongation and the extrapolation with the aid of the Hockett-Sherby approach thereafter.

Optimization procedure

In Fig. 9 an overview of the optimization procedure is given. As described in the previous section the optimization process contains only two parameters for the yield curve extrapolation. By following this approach the shape of the yield surface and the flow rule are regarded as sufficiently close to the real constitutive behavior in order to find appropriate parameters for the two remaining Hockett-Sherby parameters *c* and *n*. In a broader sense this leads to the conclusion that the model that is set up shall contain enough degrees of freedom within its spatial and physical representation of the problem to find a suitable set of parameters that allows correlation to the experiment. This means, that an approach with an isotropic constitutive model may fail for a material with orthotropic behavior. It is obvious that an optimization procedure will not necessarily deliver a convergent result in this case. Consequently one has to make sure that the applied model (spatial discretization

and constitutive representation) incorporates the correct dimensions and size of the design space in order to allow for a successful optimization.

So the optimization procedure is based on the experimental tensile tests with their optical evaluation by the DIC system and on the simulation of the tensile test strain field computed and evaluated with LS-DYNA®.
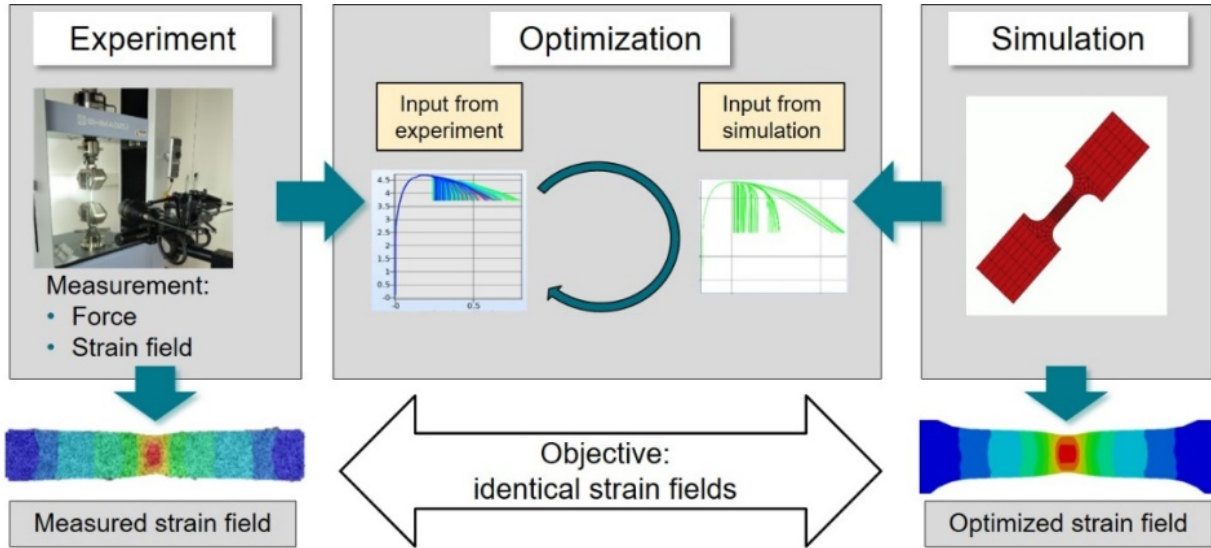

Figure 9: Overview of the optimization process.

From the experimental investigation the tensile force vs. strain curves of all facet points located in the evaluation domain are exported. This family of curves is imported into LS-OPT and serves as an optimization target for the force vs. strain curves obtained through the simulation. The two parameters *c* and *n* used in the modified Hockett-Sherby extrapolation approach of the yield curve are optimization variables; they are both constant within the discretized domain. After each optimization loop a comparison of the deformation fields between simulation and experiment delivers information about the correlation between the numerical model and the experimental reality. However, before the two strain fields can be compared in detail a spatial transformation may be necessary in order to align the surface and the orientation. This procedure is supported by the LS-OPT user interface. Furthermore, the DIC data of the evaluation domain needs to be aligned with the coordinates and loading stages of the simulation. This alignment of the deformed domain is calculated using a least squares formulation which assigns any number of test points X_{Test} to corresponding coordinates on the finite element mesh X_{FE}:

$$\min_{\boldsymbol{T}} \|X_{Test}\boldsymbol{T} - X_{FE}\|$$

These two sets of points do not have to correspond exactly as the alignment is based on the least squares principle which will minimize the fitting error. The solution of the equation yields the transformation matrix $\boldsymbol{T}$ which is subsequently used to transform all the test points into the coordinate system of the simulation. The force vs. strain data of the facet points are used in the optimization procedure to evaluate the correlation (or deviation) between simulation and experiment. Hence, the classical optimization task may be written as

$$f(\boldsymbol{x}) = \sum_{j=1}^{N} \left\| \boldsymbol{\varphi}_j(\boldsymbol{x}) - \widetilde{\boldsymbol{\varphi}}_j \right\|^2$$

where the parameters *c* and *n* are optimized such that the deviation $f(\boldsymbol{x})$ between the measured strain field and the computed strain field reaches a minimum [14].

Here, the solution vector $\boldsymbol{\varphi}_j(\boldsymbol{x})$ includes strains or alternatively displacements of the facet points at the load stages *j* while *N* represents the overall number of load stages. The vector $\boldsymbol{x}$ represents the unknown material parameters. From this the values of the simulation $\widetilde{\boldsymbol{\varphi}}_j$ with an identical number of nodes are subtracted. This

formulation can be arbitrarily extended by the curves obtained in the optical full-field measurement such as the global force vs. strain curves.

Examples

Tensile specimen were milled out along the rolling direction from a 1.25mm thick steel sheet of CR210IF to prove the concept of the above discussed full-field calibration approach. The first example shows an optimization using the isotropic MAT_024 material model. In addition, a parameter identification based on an anisotropic material model according to Barlat, in particular MAT_036, was performed [14 &15]. For this purpose further tensile specimens were taken at 45° and 90° with respect to the rolling direction.

Application of MAT_PIECWISE_LINEAR_PLASTICITY (MAT_024)

Fig. 10 shows the DIC contour plot of the strain in the x-direction, which is along the longitudinal (rolling) direction, taken from the DIC software system. Furthermore, evolution plots of force vs. strain in the x-direction within the domain of interest are depicted. Each curve represents a facet midpoint resulting from the optical measurement. The left-hand side of the screen shows the user interface with which the user is able to control different load stages and images of the optical measurement system [13].
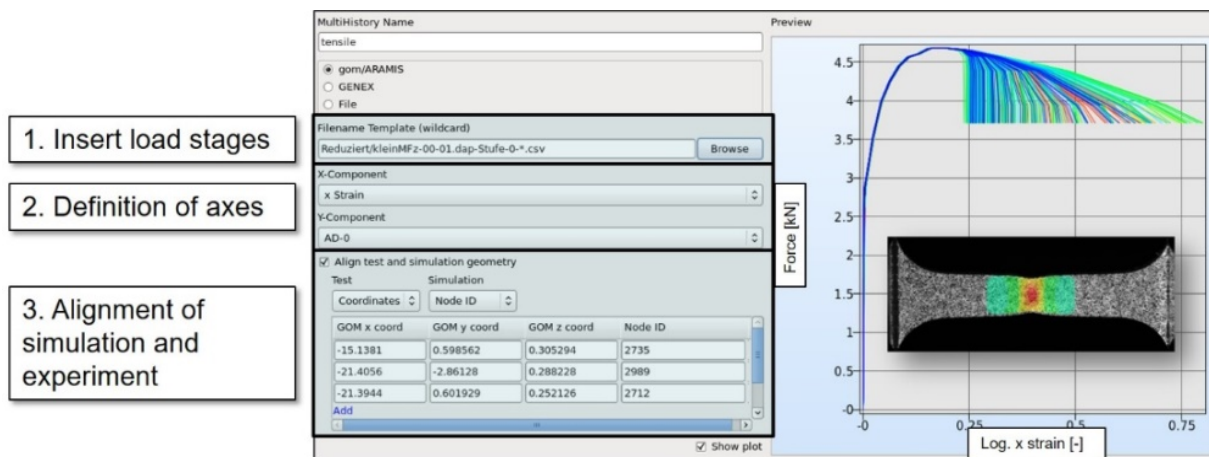

Figure 10: DIC Interface in LS-OPT showing alignment input and verification plot of selected force vs. x strain curves.

For the optimization, the parameters *c* and *n* of the Hockett-Sherby extrapolation served as optimization variables. The optimization goal was chosen to be the minimal distance of the functional $f(x)$ which describes the correspondence of the calculated nodes and the measured facet points in each deformation state. The optimization was conducted using the Feedforward neural network method (FFNN) of LS-OPT [1].

Fig. 11 shows the meta-model after the optimization with the FFNN. The point with the smallest value of the distance function returns the values for *c=0.616* and *n=0.299*. These parameters lead to the yield curve shown on the right side of Fig. 11. For comparison this figure also shows the yield curve created via the conventional method, which means that the curve was created on the basis of a fixed reference length.

Fig. 12 compares the strain fields in x-direction between the optical measurement from the experiment with the optimization based on the full-field calibration (FFC) method and the classical method. The comparison shows that the optimization by the FFC method captures the strain field of the experimental investigation better than the conventional method, in which the optimization is based only on a fixed reference length. However, major improvements are expected once a non-isotropic behavior is regarded.
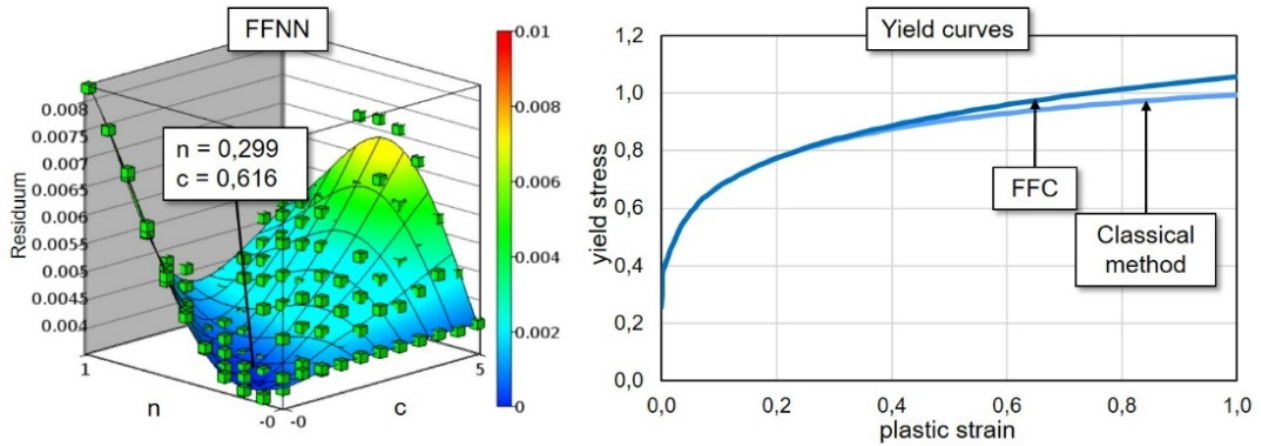
Figure 11: Meta-model after the optimization with the feedforward neuronal network (left). Comparison of the yield curves created with the full-field calibration method and the classical method (right).
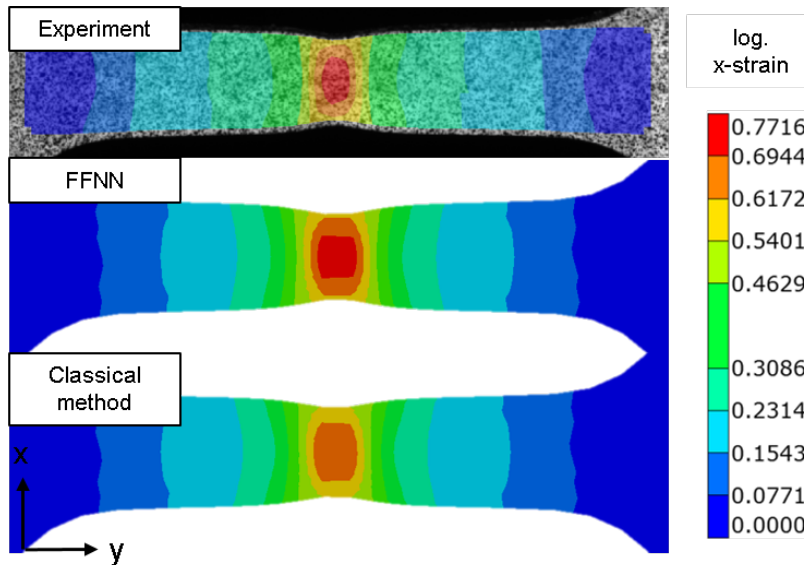

Figure 12: Comparison of the x-strain plots obtained from the DIC evaluation (top), the optimization based on the FFC method (middle) and the conventional method (bottom).

Application of MAT_3-PARAMETER_BARLAT (MAT_036)

Fig. 13 shows the DIC contour plots of the strains in x- and y-direction (right and left column) and with 0°, 45° and 90° to the rolling direction (top to bottom) visualized by the DIC software system. Furthermore force vs. x- and y-strain curve plots within the domain of interest are depicted. The left-hand side of the screen shows the contour plots of the y-strain and the force vs. y-strain curves while the right-hand side shows the contour plots of the x-strain and the force vs. x-strain curves.

For the optimization, the parameters c and n of the Hockett-Sherby extrapolation for every rolling direction served as optimization variables. In contrast to the optimization with MAT_024 (see above), this leads to six optimization variables, two for each rolling direction. Another difference to the previous example with MAT_024 are the force vs. y-strain curves which are additionally used as an optimization target. The optimization was conducted using the sequential response surface method (SRSM) with domain reduction of LS-OPT [1]. Fig. 14 shows the evolution of the force vs strains in x- and y-direction, respectively, of the experiment and the resulting curves of the simulation after one (blue curves) and 15 iterations (red curves). The

optimization by the FFC method indicates that the simulated curves are already close to the curves of the experiment.
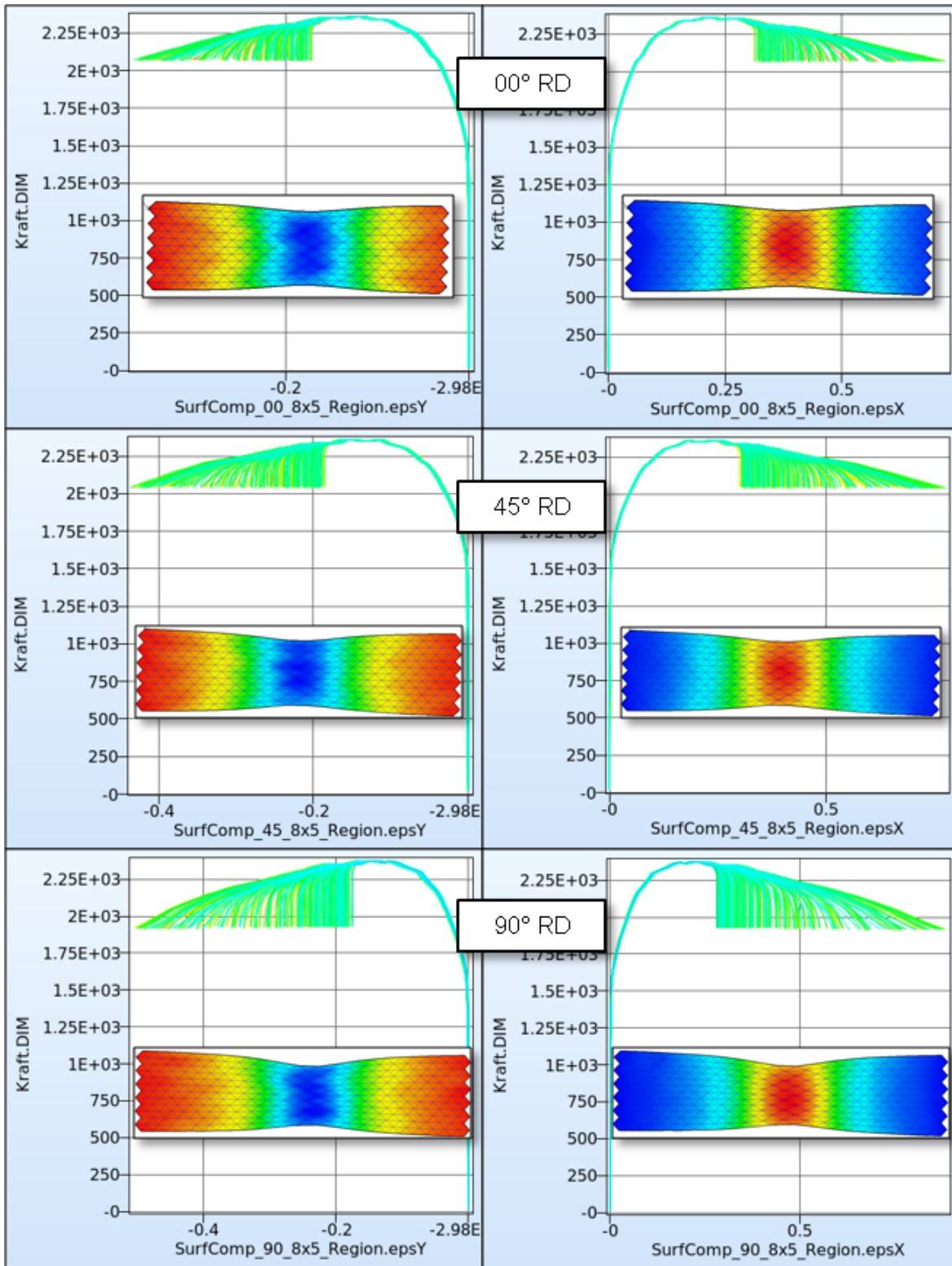

Figure 13: DIC input for the optimization with MAT_036 showing fringe plots of the tensile tests in 0°, 45° and 90° with respect to the rolling direction and the respective force-strain curves.
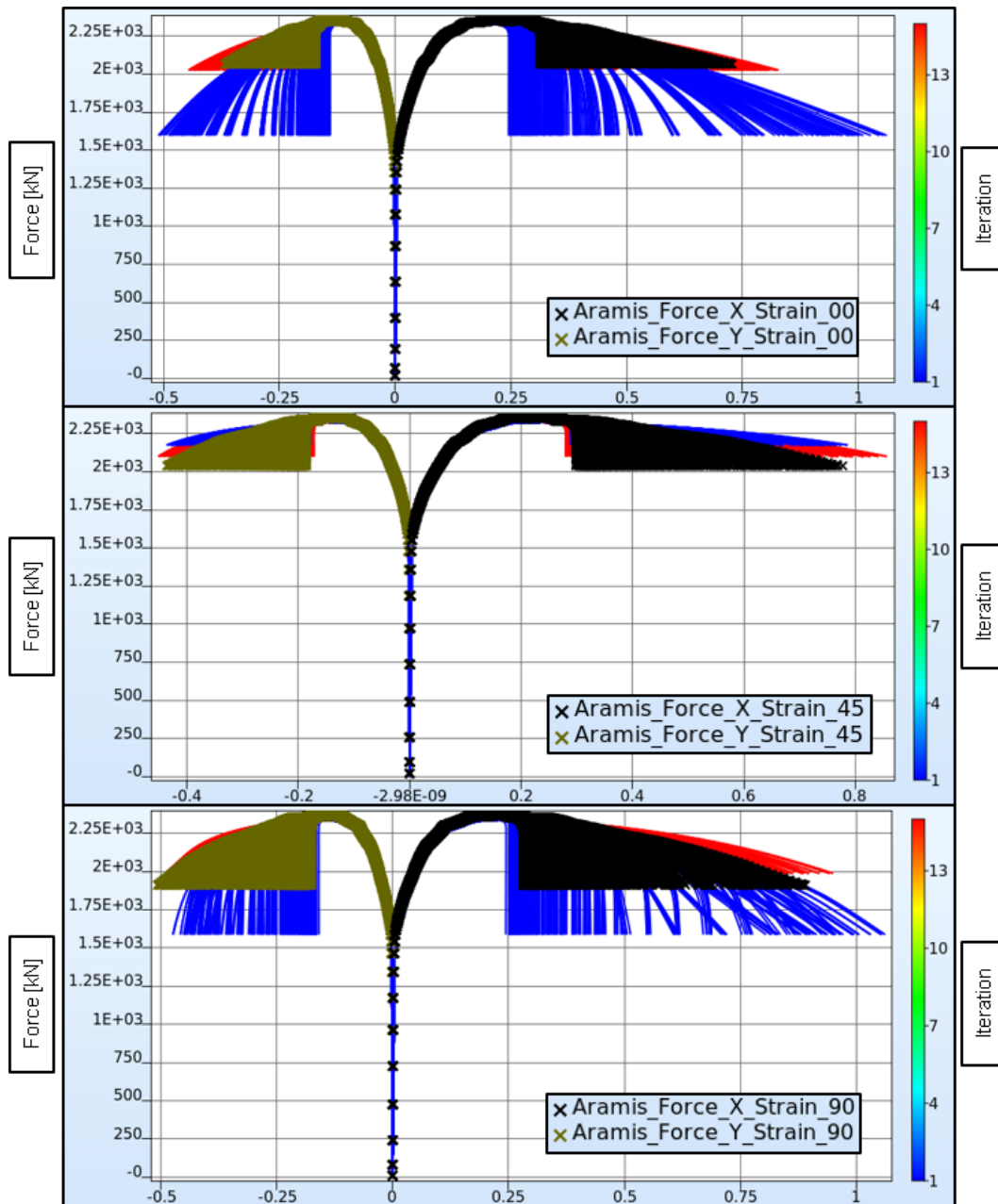
Figure 14: DIC input and the simulated force vs. x/y strain curves after one (blue) and 15 iterations (red) of the tensile tests/simulations in 0°, 45° and 90° with respect to the rolling direction.

Conclusions

In the present study, a parameter-identification procedure was carried out for the yield curve extrapolation according to a modified Hockett-Sherby extrapolation based on the optical full-field measurement in the uniaxial stress state for sheet metal of grade CR210IF.

For the optimization with LS-OPT and the isotropic MAT_024 constitutive model, a finite element simulation model based on the STL output of the applied DIC system was set up. The parameters c and n, which determine the shape of the yield curve extrapolated from the point of uniform elongation, served as optimization variables. The optimization was based on the load stages exported from the DIC software with the force vs. strain values

of individual facet points. On the basis of this optimization target, and the variables *c* and *n*, a numerical optimization scheme was carried out using the FFNN method in LS-OPT.

In addition, a parameter identification was performed using the classical method based on a fixed reference length of 10mm. The comparison of the longitudinal strain just before fracture of the sample shows that the optimization by means of the proposed full-field calibration method is able to better capture the strain field w.r.t. the experimental data. This holds especially in regions with strong localization, i.e. necking, when compared to the classical extrapolation method.

Furthermore, parameter identification for the anisotropic material model MAT_036 was performed. Again, the parameters *c* and *n* for 0°, 45° and 90° to the rolling direction functioned as optimization variables. In addition to the first example, the optimization was based not only on the force vs. x-strain curves but also on the force vs. y-strain curves. Due to the greater number of optimization variables the faster SRSM method of LS-OPT was used.

Based on the findings of the present work, it can be stated that the FFC method represents a good alternative for the identification of the parameters of the yield curves. The second example gave a little insight into the many optimization possibilities of this new method. In the future, an additionally approach of numerical optimization of the Lankford parameters will be tested using an appropriate constitutive model.

In addition, in the present work the extrapolation function according to Hockett-Sherby provides only a limited design space with only two optimization variables. Therefore, other ways to extrapolate the yield curve could be used, such as combined extrapolation functions or even spline functions. Moreover, the work is currently under way to visualize the deviation of both strain fields in LS-PrePost, which would allow a much more detailed investigation of the results.

References

[1]   Stander N., Witowski K., Ilg C.,Haufe A., Helbig M., Koch D. Application of Digital Image Correlation to Material Parameter Identification using LS-OPT, 11th European LS-DYNA Conference, Salzburg, 2017.

[2]   Stander N., Craig K.J., Müllerschon H., Reichert R. Material Identification in structural optimization using response surfaces, Structural ans Multidisciplinary Optimization, Volume 29, Issue 2, pp. 93-102, 2005.

[3]   Flores P., Tuninetti V., Gilles G., Gonry P., Duchêne L., Habraken A. Accurate stress computation in plane strain tensile tests for sheet metal using experimental data, Journal of Materials Processing Technology, pp. 1772-1779, 2010.

[4]   Kleuter B., Bosseler M. Parameteridentifikation für nichtlineare Materialmodelle in der FEM mittels optischer Verformungsanalyse, NAFEMS Magazin, Ausgabe 12, 2009.

[5]   Küsters N., Brosius A. Semi-analytic parameter identification for complex yield functions, MATEC Web of Conferences, Vol. 80, EDP Sciences, 2016.

[6]   Chaparro B.M., Thullier S., Menezes L.F., Manach P.Y., Fernandes J.V. Material parameters identification: Gradient-based, genetic and hybrid optimization algorithms, Computational Materials Science 44, pp. 339-346, 2008.

[7]   Avril S., Bonnet M., Bretelle A.-S., Grédiac M., Hild F., Ienny P., Latourte F., Lemosse D., Pagano S., Pagnacco E., Pierron F. Overview of identification methods of mechanical parameters based on full-field measurements, Experimental Mechanics, pp. 1-40, 2008.

[8]   Grédiac M., Pierron F. Applying the Virtual Fields Method to the identification of elasto-plastic constitutive parameters, International Journal of Plasticity 22, pp. 602-627, 2006.

[9]   Kim J.-H., Serpantié A., Barlat F., Pierron F., Lee M.-G. Characterization of the post-necking strain hardening using the virtual fields method, International Journal of Solids and Structures 50, pp. 3829-3842, 2013.

[10] DIN EN ISO 6892-1 Metallische Werkstoffe – Zugversuch – Teil 1: Prüfverfahren bei Raumtemperatur, 2009.

[11] Winter D. Optische Verschiebungsmessung nach dem Objektrasterprinzip mit Hilfe eines flächenorientierten Ansatzes, Dissertation, Universität Braunschweig, 1993.

[12] Hockett J.E., Sherby O.D. Large Strain deformation of polycrystalline metals at low homologous temperatures, Journal of the Mechanics and Physics of Solids 23, pp. 87-98, 1975.

[13] Stander N., Roux W.J., Basudhar A., Eggleston T., Craig K.-J. LS-OPT Users Manual, Version 5.2., December 2015.

[14] Mahnken, R., Stein, E. Parameter Identification for Finite Deformation Elasto-Plasticity in Principal Directions, *Comput. Methods Appl. Mech. Engrg*, 147, 17-39, 1997.

[15] Hallquist, J.O. *LS-DYNA Users Manual Volume II, Livermore Software Technology Corporation.*

[16] Barlat F., Lian J. Plastic behavior and stretchability of sheet metals, Part I: A yield function for orthotropic sheets under plane stress conditions, International Journal of Plasticity 5, pp. 51-66, 1989.